



Highly durable and flexible memory based on resistance switching

Sungho Kim, Oktay Yarimaga, Sung-Jin Choi, Yang-Kyu Choi ^{*,1}

School of Electrical Engineering and Computer Science, KAIST, Daejeon 305-701, Republic of Korea

ARTICLE INFO

Article history:

Received 15 April 2009

Received in revised form 24 August 2009

Accepted 25 October 2009

Available online 24 November 2009

The review of this paper was arranged by Dr. Y. Kuk

Keywords:

Flexible

Resistance random access memory

γ -Irradiation

ABSTRACT

Resistance random access memory (RRAM) consisting of stacked Al/TiO_x/Al structure is demonstrated on a flexible and transparent substrate. To improve cell to cell uniformity, TiO_x formed by atomic layer deposition is used for resistive switching material. The simple cross-bar structure of the RRAM and good ductility of aluminum electrode results in excellent flexibility and mechanical endurance. Particularly, bipolar and unipolar resistive switching (BRS, URS) behavior appeared simultaneously were investigated. Depending on the current compliance, BRS or URS could be selectively observed. Furthermore, the permanent transition from BRS to URS was observed with a specific current compliance. To understand this transition behavior, the γ -ray irradiation effect into resistive switching is primarily investigated.

© 2009 Elsevier Ltd. All rights reserved.

1. Introduction

Many flexible devices have been developed for electronic paper, transistors for displays, sensors, solar cells, and organic light emitting diodes [1–3]. Based on this technological trend, the need for a flexible type of memory will also increase to support these flexible electronic devices, similar to the role of flash memory in solid state electronics today. However, most types of flexible memories have been based on organic materials [4–6]. Although organic memory shows good flexibility, its performance cannot match that of conventional flash memory. Additionally, the fabrication process of organic memory is complicated by the requirements of controlled external conditions. These limitations require additional efforts to improve memory performance and increase processing costs.

Recently, resistance random access memory (RRAM) has attracted great attention due to its potential to replace flash memory in next-generation nonvolatile memory applications [7,8]. The resistive switching effect is observed as a result of various insulating materials that consist of CMOS process compatible inorganic materials. In addition, the current–voltage (I – V) characteristics of the simple metal–insulator–metal (MIM) structure exhibit rapid switching speeds and distinctive changes of the resistance between the high resistance state (HRS) and the low resistance state (LRS).

In the present study, the fabrication of a flexible type of RRAM is reported. In an earlier work by the authors, plasma oxidized alumi-

num [9] and sol–gel derived zinc oxide [10] were used as resistive switching material for flexible type RRAM. On the other hand, in this study, atomic layer deposition (ALD) process is used to improve cell to cell uniformity and for realistic feasibility in flexible memory applications using existing semiconductor technology. The structural simplicity and good ductility of aluminum electrode result in advantages that include good flexibility, mechanical endurance, and durability. In addition, the resistive switching mechanism is investigated by means of a permanent transition from bipolar resistive switching (BRS) to unipolar resistive switching (URS) in TiO_x films, as understood through γ -ray irradiation effects.

2. Device fabrication

The flexible RRAM was fabricated on the flexible and transparent substrate of polyethersulfone (PES), as shown in Fig. 1. The PES film was glued onto a silicon wafer with polyimide. Aluminum with a thickness of 150 nm was used for the top and bottom electrodes. The electrodes were patterned by conventional photolithography ranging from 2×2 to $100 \times 100 \mu\text{m}^2$. TiO_x of 10 nm thickness was used to formulate the resistive switching material. The TiO_x films were deposited using plasma-enhanced atomic layer deposition at 180 °C. The process temperature of the deposition is limited by the maximum working temperature of PES, which is 200 °C. The thicknesses of the deposited films were confirmed by transmission electron microscopy images. The silicon wafer served only as a mechanical support during the processing stage; it was subsequently peeled off manually after the fabrication of the flexible RRAM.

* Corresponding author.

E-mail addresses: kkam226@gmail.com (S. Kim), ykchoi@ee.kaist.ac.kr (Y.-K. Choi).

¹ Tel.: +82 42 350 3477; fax: +82 42 350 8565.

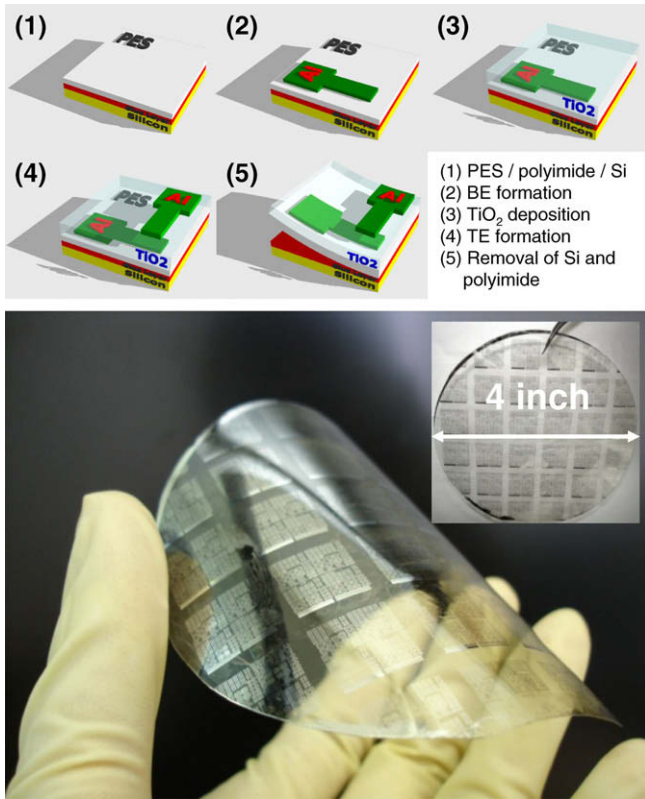


Fig. 1. The process flow of flexible RRAM and a photograph of flexible RRAM.

3. Resistive switching mechanism

3.1. Switching performance

Fig. 2a shows the typical switching characteristics of Al/TiO_x/Al that produces BRS. Bias sweeps were conducted in the direction 0 V → -3 V → 0 V → 3 V → 0 V. The current increased sharply at a negative bias (V_{SET}) and switched from HRS to LRS. The LRS remains during the voltage sweep back at a positive bias less than V_{RESET} . The resistance ratio (R_{off}/R_{on}) between HRS and LRS is larger than 50 at $V_{READ} = 0.2$ V under a compliance current of 500 μ A. Fig. 2b shows the measured retention characteristics of the fabricated Al/TiO_x/Al devices in the HRS and in the LRS. No significant changes of the resistance in either case were observed after 10^4 s at 85 °C. Additionally, the reliable endurance showing a sustained resistance ratio larger than 50 is achieved even after switching cycles of 10^5 times, as shown in Fig. 2b.

On the one hand, one interesting phenomenon was observed that both BRS and URS could be appeared in TiO_x films depending on the current compliance. TiO_x films show the BRS mode at a low current compliance (<500 μ A) while revealing the URS mode at a high current compliance (>10 mA) after electroforming process, as shown in Fig. 3a. Furthermore, a permanent transition from BRS to URS was observed when a high current (~3 mA) was applied. After the transition of the switching mode, the R_{off}/R_{on} value and distribution changed dramatically, as shown in Fig. 3b.

3.2. Oxygen vacancies in TiO_x

The inset of Fig. 2a shows a logarithmic plot of the I - V characteristics of TiO_x films for BRS mode. In the low-voltage region, the current is linearly proportioned to the voltage ($I \propto V$), which is followed by $I \propto V^2$. The $I \propto V^2$ correlation can be understood as the ef-

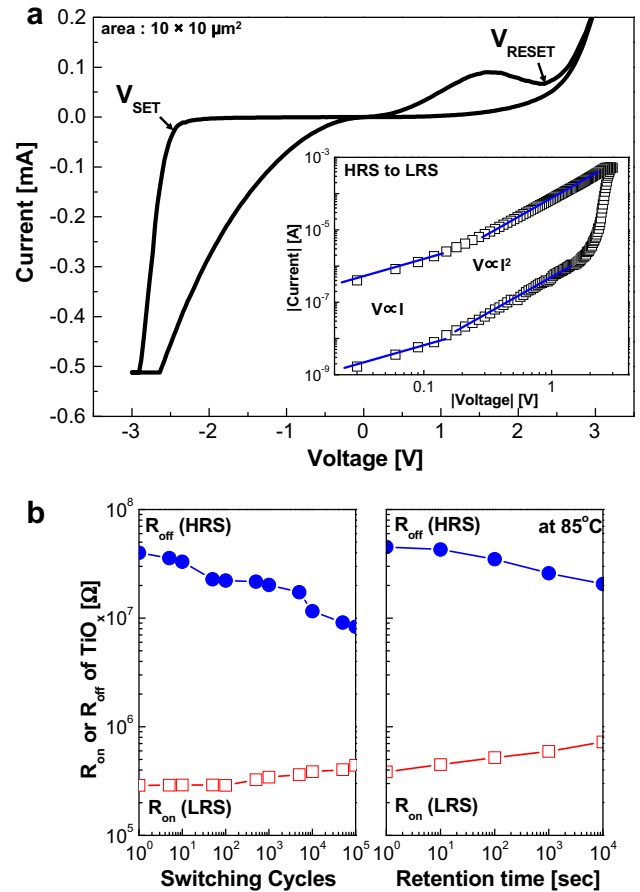


Fig. 2. (a) Typical I - V curve of an Al/TiO_x/Al device. The inset represents I - V characteristics for Fig. 2a in a double-logarithmic plot. (b) Endurance test under the current compliance of 500 μ A. In addition, data retention characteristics for HRS and LRS; the resistance values in HRS and LRS were read at 0.2 V at 85 °C.

fect of the space-charge-limited current (SCLC) [11–13]. From a previous analysis by the authors [14], it was verified that the resistive switching of Al/TiO_x/Al device was governed by SCLC in the only TiO_x layer near the top electrode. However, a suitable physical analysis of TiO_x film could not be provided.

To carry out further detail analysis for resistive switching, Fig. 4a shows a transmission electron microscope (TEM) image of the fabricated Al/TiO_x/Al device. As shown in Fig. 3a, a TiO_x layer with a thickness of 10 nm was deposited initially. However, between the top electrode and the TiO_x layer, another layer (~5 nm) was newly generated. To identify this layer, a transmission electron microscope-energy dispersive X-ray spectrometry (TEM-EDX) analysis was carried out. Fig. 4b shows the scanned atom profiling between top and bottom electrode by TEM-EDX analysis. From this data, it is found that an oxygen-deficient layer was preferentially produced in the TiO_x layer near the top electrode naturally. It was also observed that some fraction of the aluminum in the top electrode diffused into the TiO_x layer. The newly generated layer (the oxygen-deficient layer) can be considered as an Al-doped TiO_x layer. For the Al-doped TiO₂, Al³⁺ substitutes for Ti⁴⁺ within the TiO_x, and oxygen vacancies can be produced by diffused Al³⁺ [15]. It is improbable that an Al³⁺ ion in TiO_x acts as a trap and captures an electron; instead, an oxygen vacancy traps an electron [16,17].

Therefore, the mechanism of BRS mode can be speculated that oxygen vacancies in the TiO_x layer near the top electrode act as traps for electrons as shown in Fig. 5a. During SET process, injected electrons from the top electrode are filled oxygen vacancies and

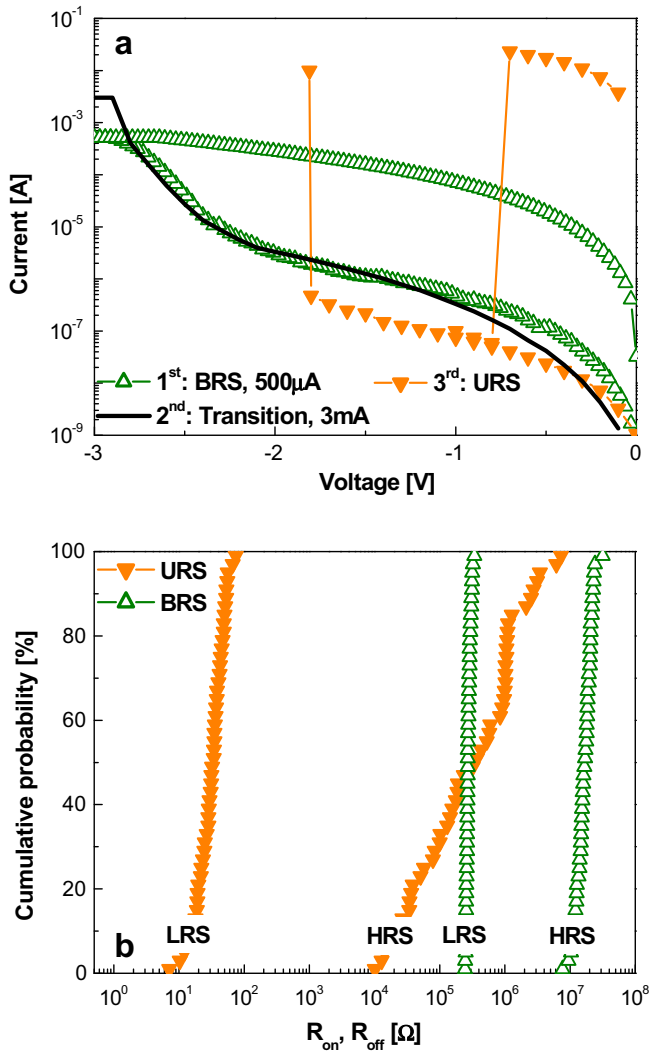


Fig. 3. (a) The switching mode transition depends on the compliance current level in TiO_x films. (b) R_{on} and R_{off} distribution in both the BRS and URS modes.

oxygen ions move to the bottom electrode, which generates the additional oxygen vacancies. Consequently, distributed oxygen vacancies induce trap-controlled SCLC and dominantly contribute to the resistive switching. On the other hand, in the case of HRS mode, defects such as oxygen vacancies tend to be aligned to form tiny conducting filaments in the bulk region after electroforming process [18], as shown in Fig. 5b. Although primary oxygen vacancies are localized near the top electrode, oxygen vacancies are re-distributed or some defects are newly generated due to the high electric field during electroforming process. These tiny conducting filaments gather together to form stronger and more conducting filaments, which lead to the transition to the LRS. During RESET process, electrons are depleted in some oxygen vacancies (especially near the top electrode) and electron-depleted oxygen vacancies are recombined with O^{2-} . It has been still in controversy that the HRS current of the URS mode may be transported through the oxide films through hopping conduction [19], Poole–Frenkel emissions [20], or by the space-charge-limited current [21].

3.3. BRS and URS transition and mechanism

Permanent switching mode transition, BRS–URS, according to the current compliance, has been reported elsewhere [22,23] that

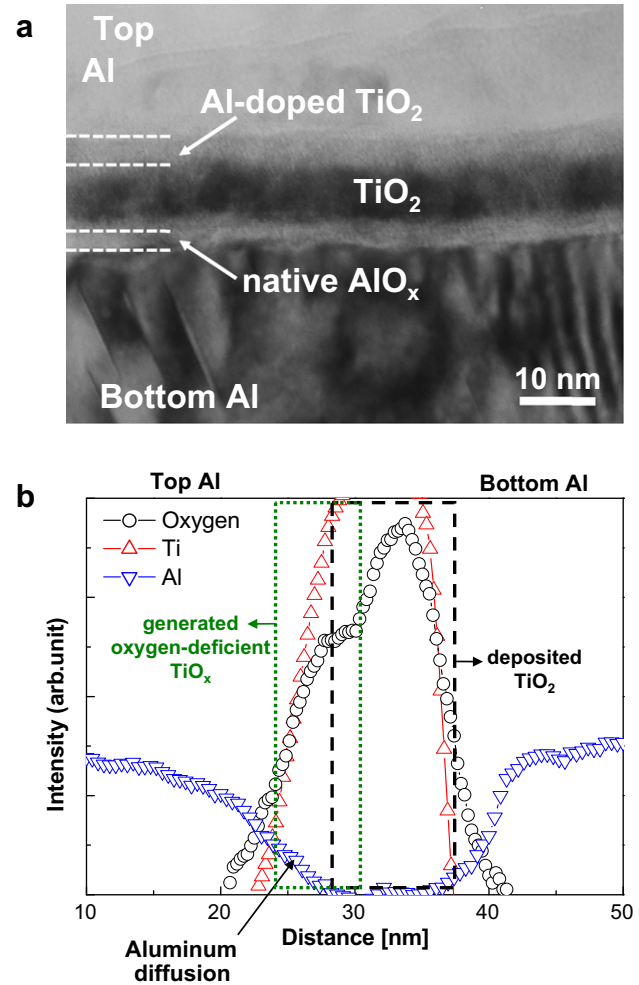


Fig. 4. (a) Transmission electron microscopy image of the Al/ TiO_x /Al structure. (b) TEM-EDX depth profiling data. An oxygen-deficient layer is induced by the active-top aluminum.

it was observed restrictedly in titanium oxide material. The first observation of the transition characteristic was reported by Jeong et al. in Pt/ TiO_2 /Pt stack [22]. At that time, however, the only observation of transition was reported and physical analysis was not provided. More intensive analysis was carried out by Wang et al. using analyses of correlation between RESET condition and R_{on} [23]. From correlation between RESET current and R_{on} , the URS mode of TiO_x was in accordance with the thermal dissolution model [24], which states that, the conductive filament was thermally destroyed by current crowding and local heating effects during RESET. In addition, the BRS mode of TiO_x can be understood from correlation between RESET voltage and R_{on} by the redox-reaction model [25]. It implies that resistive switching is caused by a local electrochemical redox reaction near the top electrode (anode) interface. These explanations are well consistent with aforementioned switching mechanism of Al/ TiO_x /Al device.

In this work, to investigate transition characteristic from BRS to URS in detail, γ -irradiation technique was introduced. The total irradiation dose was 100 krad with a dose rate of 50 rad/s. The resistive switching of the TiO_x films was performed in the BRS mode at first. Then, γ -ray was irradiated into the device with ^{60}Co . Lastly, the URS mode was achieved after mode transition at 3 mA current compliance. The device which showed a transition BRS to URS without γ -irradiation was also investigated as a control group. Fig. 6a shows experimental results that modulation of R_{on}

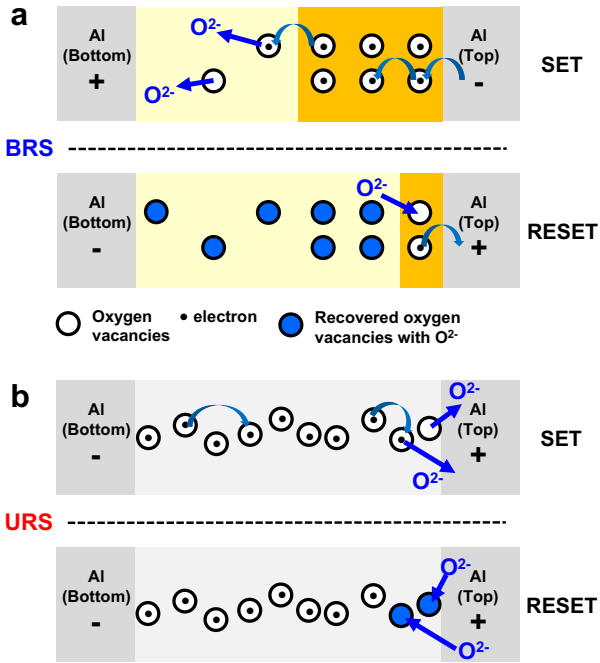


Fig. 5. (a) The schematic diagram for the mechanism of BRS mode. (b) The schematic diagram for the mechanism of URS mode.

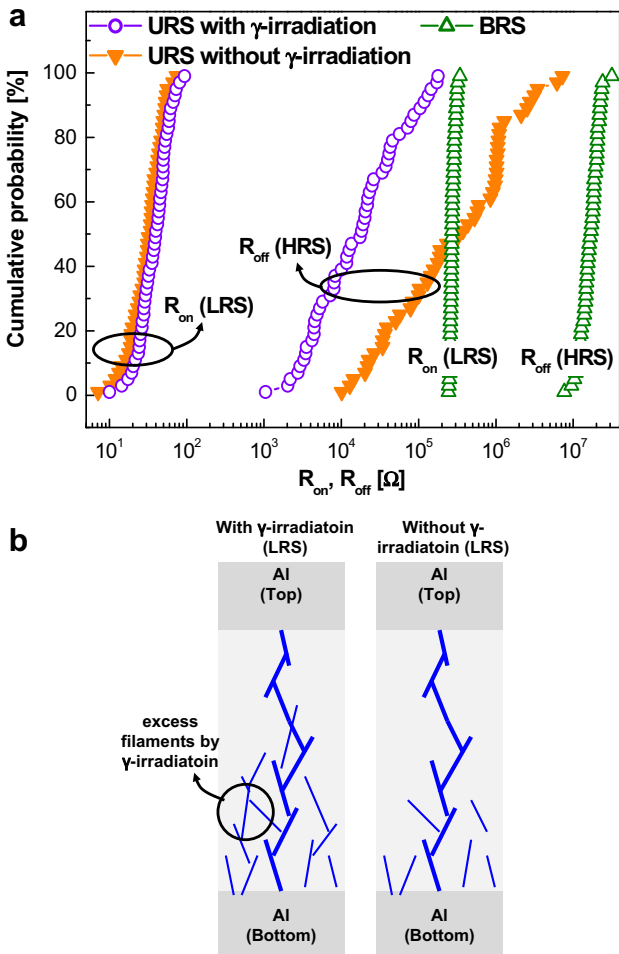


Fig. 6. (a) Irradiation effect of the R_{on} and R_{off} distribution. (b) The schematic diagram for the expected filaments formation with and without γ -irradiation.

and R_{off} in a comparison made with and without γ -irradiation in the URS mode. In the case of the URS mode with γ -irradiation, only R_{off} was decreased after switching mode transition. It was known that the valence of the Ti ion varies after irradiation that the Ti^{3+} ion increases in contrast with the Ti^{4+} ion decreases [26]. A fraction of Ti^{4+} ions turns to Ti^{3+} ions and the chemical composition changes as $2TiO_2 + 2e^- \rightarrow Ti_2O_3 + O^{2-}$, hence excess oxygen ions (O^{2-}) and oxygen vacancies are created in the irradiated layer.

Consequently, more conducting filaments are formed by γ -ray induced excess oxygen ions when the switching mode transition was occurred because defects such as oxygen vacancies tend to form conducting filaments. In the case of LRS in the URS mode, there is no significant change between with and without γ -irradiation. It can be understood that excess filaments has not an important role for current flowing because current mainly flow through the main filaments which connect both electrodes, as shown in Fig. 6b (expected filaments formation is referred to simulation results by random circuit breaker network model [27]). However, in the case of HRS in the URS mode, remained excess filaments cause the leakage current path, so R_{off} is decreased. This behavior from excess filaments is equivalent to the cell area dependency of the HRS and LRS in URS mode. Generally, in the case of URS, R_{off} increases as the cell area decreases, whereas R_{on} is independent of the cell area. It implies that larger cell area device has the more ex-

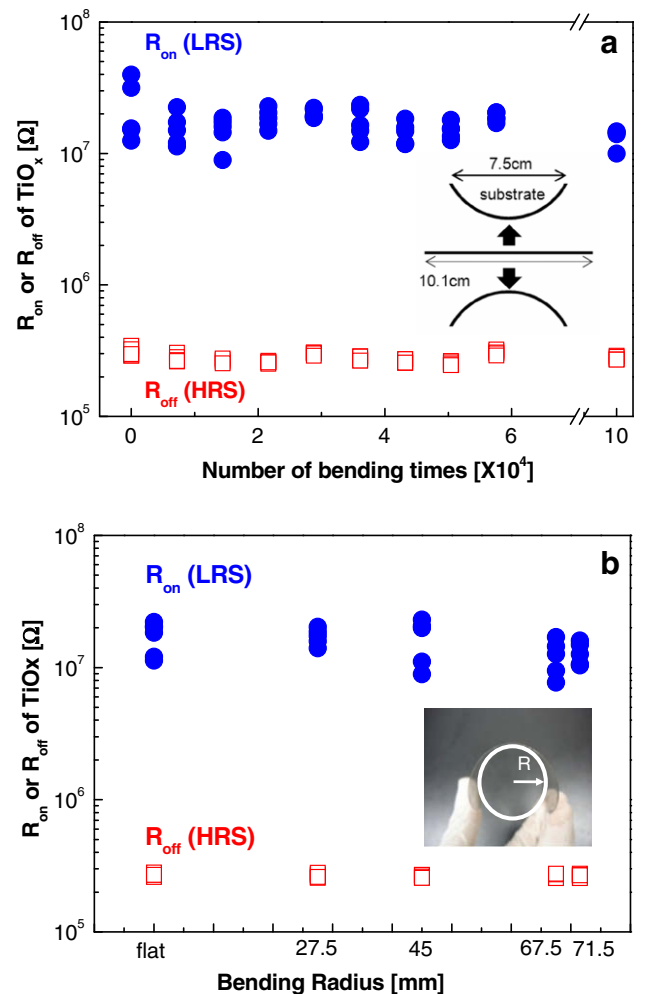


Fig. 7. All data; five different randomly selected devices were measured each time. (a) The switching characteristics with continuous bending of a PES substrate at a reading voltage of 0.2 V. (b) The current ratio between the on and off states as a function of the bending radius at a reading voltage of 0.2 V.

cess filaments, so more leakage current path reduces R_{off} . Therefore, during switching mode transition, oxygen ions and vacancies are redistributed and formed conducting filaments due to the enough energy from the high compliance current. During this process, the amount of oxygen ions and vacancies determines the behavior of resistive switching after transition.

4. Flexibility and mechanical endurance

Good mechanical flexibility is crucial for applications in flexible electronics. The level of mechanical endurance was evaluated by performing a substrate bending test in which both tensile and compressive stresses were induced, as shown in Fig. 7a. A vibrator was used to induce substrate bending 4 times/s for the total of 10^5 bends. Even at 10^5 bends, the $R_{\text{off}}/R_{\text{on}}$ value was unchanged. In addition, the devices exhibited good flexibility, as shown in Fig. 7b. In the flexibility test, severe bending of the device did not affect memory performance. These results indicate that the switching characteristics of flexible RRAM are independent of device bending due to the good ductility of the aluminum electrode and the mechanical endurance arising from the simple device structure.

5. Conclusions

RRAM device was fabricated and showed reliable endurance and retention characteristics, even on a flexible substrate. The transition behavior from BRS to URS was understood with the aid of γ -irradiation. This flexible type of RRAM is attractive for low-cost and wearable devices and may be suitable in flexible displays.

Acknowledgements

This research was supported by a Grant (08K1401-00210) from the Center for Nanoscale Mechatronics & Manufacturing, one of the 21st Century Frontier Research Programs supported by the Korea Ministry of Education, Science and Technology (MEST).

References

- [1] Chen Y, Au J, Kazlas P, Ritenour A, Gates H, McCreary M. Electronic paper: flexible active-matrix electronic ink display. *Nature* 2003;423:136.
- [2] Ju S, Facchetti A, Xuan Y, Liu J, Ishikawa F, Ye P, et al. Fabrication of fully transparent nanowire transistors for transparent and flexible electronics. *Nat Nanotechnol* 2007;2:378–84.
- [3] Mcalpine MC, Ahmad H, Wang D, Heath JR. Highly ordered nanowire arrays on plastic substrates for ultrasensitive flexible chemical sensors. *Nat Mater* 2007;6:379–84.
- [4] Li L, Ling QD, Lim SL, Tan YP, Zhu C, Chan DSH, et al. A flexible polymer memory device. *Org Electron* 2007;8:401–6.
- [5] Moller S, Perlov C, Jackson W, Taussig C, Forrest SR. A polymer/semiconductor write-once read-many-times memory. *Nature* 2003;426:166–9.
- [6] Naber RCG, Tanase C, Blom PWM, Gelinck GH, Marsman AW, Touwslager FJ, et al. High-performance solution-processed polymer ferroelectric field-effect transistors. *Nat Mater* 2005;4:243–8.
- [7] Zhuang WW, Pan W, Ulrich BD, Lee JJ, Stecker L, Burmaster A, et al. Novel colossal magnetoresistive thin film nonvolatile resistance random access memory (RRAM). In: IEDM technical digest, vol. 2; 2002. p. 193–6.
- [8] Baek IG, Lee MS, Seo S, Lee MJ, Seo DH, Suh DS, et al. Highly scalable non-volatile resistive memory using simple binary oxide driven by asymmetric unipolar voltage pulses. In: IEDM technical digest, vol. 1; 2004. p. 587–90.
- [9] Kim S, Choi YK. Resistive switching of aluminum oxide for flexible memory. *Appl Phys Lett* 2008;29:223508.
- [10] Kim S, Moon H, Gupta D, Yoo S, Choi YK. Resistive switching characteristics of sol-gel zinc oxide films for flexible memory applications. *IEEE Trans Electron Dev* 2009;56:696–9.
- [11] Dong R, Lee DS, Xiang WF, Oh SJ, Seong DJ, Heo SH, et al. Reproducible hysteresis and resistive switching in metal-Cu_xO-metal heterostructures. *Appl Phys Lett* 2007;90:042107.
- [12] Xia Y, He W, Chen L, Meng X, Liu Z. Field-induced resistive switching based on space-charge-limited current. *Appl Phys Lett* 2007;90:022907.
- [13] Lampert MA, Mark P. *Current injection in solids*. New York: Academic; 1970.
- [14] Yu LE, Kim S, Ryu MK, Choi SY, Choi YK. Structure effects on resistive switching of Al/TiO_x/Al devices for RRAM applications. *IEEE Electron Dev Lett* 2008;29:331–3.
- [15] Gesenhues U, Rentschler T. Crystal growth and defect structure of Al³⁺-doped rutile. *J Solid State Chem* 1998;143:210–8.
- [16] Lee YC, Hong YP, Lee HY, Kim H, Jung YJ, Ko KH, et al. Photocatalysis and hydrophilicity of doped TiO₂ thin films. *J Colloid Interface Sci* 2003;267:127–31.
- [17] Gesenhues U. Al-doped TiO₂ pigments: influence of doping on the photocatalytic degradation of alkyd resins. *J Photochem Photobiol A: Chem* 2000;139:243–51.
- [18] Choi BJ, Jeong DS, Kim SK, Rohde C, Choi S, Oh JH, et al. Resistive switching mechanism of TiO₂ thin films grown by atomic-layer deposition. *J Appl Phys* 2005;98:033715.
- [19] Xu N, Gao B, Liu LF, Sun B, Liu XY, Ham RQ, et al. A unified physical model of switching behavior in oxide-based RRAM. In: VLSI symposium technical digest; 2008. p. 100–1.
- [20] Chang WY, Lai YC, Wu TB, Wang SF, Chen F, Tasi MJ. Unipolar resistive switching characteristics of ZnO thin films for nonvolatile memory applications. *Appl Phys Lett* 2008;92:022110.
- [21] Kim KM, Choi BJ, Shin YC, Choi S, Hwang CS. Anode-interface localized filamentary mechanism in resistive switching of TiO₂ thin films. *Appl Phys Lett* 2008;91:012907.
- [22] Jeong DS, Schroeder H, Waser R. Coexistence of bipolar and unipolar resistive switching behaviors in a Pt/TiO₂/Pt stack. *Electrochem Solid-State Lett* 2007;10:G51–3.
- [23] Wang W, Fujita S, Wong SS. RESET mechanism of TiO_x resistance-change memory device. *IEEE Electron Dev Lett* 2009;30:733–5.
- [24] Russo U, Ielmini D, Cagli C, Lacaita AL, Spiga S, Wiemer C, et al. Conductive-filament switching analysis and self-accelerated thermal dissolution model for reset in NiO-based RRAM. In: IEDM technical digest, vol. 1; 2007. p. 775–8.
- [25] Muraoka S, Osano K, Kanzawa Y, Mitani S, Fujii S, Katayama K, et al. Fast switching and long retention Fe–O ReRAM and its switching mechanism. In: IEDM technical digest, vol. 1; 2007. p. 779–82.
- [26] Zhang JD, Fung S, Li-Bin L, Zhi-Jun L. Ti ion valence variation induced by ionizing radiation at TiO₂/Si interface. *Surf Coatings Technol* 2002;158–159:238–41.
- [27] Chae SC, Lee JS, Kim S, Lee SB, Chang SH, Liu C, et al. Random circuit breaker network model for unipolar resistance switching. *Adv Mater* 2008;20:1154–9.